

## Expanded ensemble Monte Carlo simulations for the chemical potentials of supercritical carbon dioxide and hydrocarbon solutes

Jaecon Chang<sup>†</sup>

Department of Chemical Engineering, University of Seoul, Siripdae-gil 13, Dongdaemun-gu, Seoul 130-743, Korea  
(Received 21 May 2010 • accepted 16 June 2010)

**Abstract**—We carry out expanded ensemble Monte Carlo simulations in order to calculate the chemical potentials of carbon dioxide as solvent and those of hydrocarbons as solutes at supercritical conditions. Recently developed adaptive method is employed to find weight factors during the simulation, which is crucial to achieving high accuracy for free energy calculation. The present simulation method enables us to obtain chemical potentials of large solute molecules dissolved in compressed phase from a single run of simulation. Simulation results for the excess chemical potentials of pure carbon dioxide at 300, 325 and 350 K are compared with experimental data and values predicted by the Peng-Robinson equation of state. A good agreement is found for high pressures up to 500 bar. The chemical potentials of hydrocarbon solutes dissolved in carbon dioxide at infinite dilution are predicted by simulation. Less than eight intermediate subensembles are required to gradually insert (or delete) hydrocarbon solute molecules from methane to n-octane into dense CO<sub>2</sub> phase of approximately 1.0 g cm<sup>-3</sup>.

Key words: Molecular Simulation, Monte Carlo, Expanded Ensemble, Chemical Potential, Carbon Dioxide

### INTRODUCTION

An accurate estimation of thermodynamic properties of fluids is important to chemical process design. In engineering calculations, the thermodynamic properties have been calculated from equations of state and heat capacity data. While most cubic equations of state being used for engineering purposes are successful in correlating experimental data, they seldom reflect the details of the molecular structure of the fluids. The parameters of the equation of state often do not have clear physical meaning, and the equations of state should not be used with confidence beyond the range for which they were tested.

In the past decades, evolution of computer and progress of molecular simulation have made it possible to obtain thermodynamic properties directly from intermolecular potentials [1]. Free energies and chemical potential are of most interest to chemical engineers because they play important roles in determining phase equilibria, solubility and partitioning of solute, and the stability of fluid phase, etc. Unlike mechanical properties such as energy and pressure, these entropy-related properties do not have corresponding microscopic expressions in terms of momenta and coordinates of constituting molecules. Most simulation methods to calculate free energies are based on the ratio of partition functions, which is the difference in the free energy between two systems. Various algorithms have been developed including test particle insertion method [2], free energy perturbation method [3], thermodynamic integration method [4], acceptance ratio method [5] and expanded ensemble method [6]. Among them, the expanded ensemble method is of convenience and advantage in that the chemical potential of a large solute molecule in dense liquid phase can be efficiently calculated from a single

simulation run. There have been many simulation studies for liquids [6-14] and solids [15-18] by using expanded ensemble method combined with molecular dynamics or Monte Carlo (MC) simulations. Recently, we proposed a novel adaptive scheme [19] in which the values of weight factors are determined during the simulation from the acceptance ratio between forward and backward transitions. We demonstrated that our method combined with Monte Carlo simulation provides a reliable and convenient tool to calculate the chemical potentials of various mixtures composed of nonpolar and polar substances.

In this work, we study mixtures consisting of carbon dioxide as solvent and several nonpolar hydrocarbon solutes at supercritical conditions. We calculate PVT properties of carbon dioxide by using isothermal isobaric Monte Carlo (NPT MC) simulations and chemical potentials by using expanded ensemble Monte Carlo (EEMC) simulations. Simulation results are compared with experimental data as well as the Peng-Robinson equation of state. We discuss the effect of temperature and pressure on the excess chemical potentials of carbon dioxide and solutes, and also investigate the effect of chain length for n-alkanes.

### SIMULATION METHOD

The interatomic interactions between two atoms of species i and species j consist of the Lennard-Jones (LJ) dispersion and electrostatic terms given by

$$u_{ij}(r) = 4\epsilon_{ij} \left[ \left( \frac{\sigma_{ij}}{r} \right)^{12} - \left( \frac{\sigma_{ij}}{r} \right)^6 \right] + \frac{q_i q_j}{4\pi\epsilon_0 r} \quad (1)$$

where r is the distance between the two atoms,  $\epsilon_{ij}$  and  $\sigma_{ij}$  are LJ energy and size parameters, respectively,  $q_i$  is the partial charge of atom i, and  $\epsilon_0$  is the permittivity of vacuum. Arithmetic mean for the size parameters  $\sigma_{ij}$  and geometric mean for the energy parameters  $\epsilon_{ij}$  were

<sup>†</sup>To whom correspondence should be addressed.  
E-mail: changjae@uos.ac.kr

used for interactions between different atomic species. The LJ dispersion interactions were truncated beyond the cut-off distance of 12 Å. Standard long-range corrections contributed by the LJ interactions for the energy and pressure were taken into account during the simulation.

We used EPM2 model for carbon dioxide [20]. The EPM2 model reflects experimental quadrupole moment, and it accurately reproduces thermodynamic properties [21]. Trappe force field was used for hydrocarbon solutes as united atom models [22-24]. Solvent phases of carbon dioxide consisting of 300 CO<sub>2</sub> molecules were first prepared by carrying out isothermal isobaric Monte Carlo simulations. In Monte Carlo simulations, the magnitudes of the maximum translation and rotation were chosen to give an acceptance ratio of approximately 50%. Trial attempts of changing box size in MC simulation were done every two MC cycles. Carbon dioxide, ethane and aromatic rings were treated as rigid bodies. For flexible alkanes molecules, while bond lengths are fixed, changes in bond angles and torsion angles were attempted as frequently as the overall rotation of the molecules. The angle moves were attempted in the same manner as in our previous work [19].

Chemical potential in canonical ensemble is defined as

$$\mu = \left( \frac{\partial A}{\partial N} \right)_{T,V} \equiv A_{N+1} - A_N = -kT \ln \frac{Q_{N+1}}{Q_N} \quad (2)$$

where  $\mu$  is the chemical potential, A is the Helmholtz free energy, N is the number of molecules, k is the Boltzmann constant, and Q is the canonical partition function. Solution is composed of N solvent molecules and a solute molecule designated as the N+1-th molecule. The chemical potential of the solute at infinite dilution is a difference in the free energy between pure solvent and solution containing a solute molecule.

The partition function of the expanded ensemble is a weighted sum of individual partition functions of constituting subensembles [6]. In isothermal isochoric (NVT) condition, the expanded ensemble is written as

$$Q_E(N, V, T) = \sum_{i=0}^M \exp(w_i) Q(N, V, T; \lambda_i) \quad (3)$$

where M is the number of subensembles, Q is the partition function of a subensemble associated with the coupling parameter  $\lambda_i$ , and  $w_i$  is a corresponding weight factor. The weight factor enables biased sampling over subensembles in order that almost a uniform sampling is achieved by flattening free energy profile added by the weight factor. In MC simulations, a transition between adjacent subensembles is accepted by using the Metropolis method taking into account the weight factor:

$$P_{acc}(\lambda_i \rightarrow \lambda_j) = \min \{ 1, \exp(w_j - w_i) \exp[-\beta(U_j - U_i)] \} \quad (4)$$

where  $P_{acc}$  is the acceptance probability and  $U_i$  is the potential energy of system at  $\lambda_i$ . The difference in the weight factors is used to bias the acceptance probability of a trial transition move between subensembles, and its value is a rough estimate of free energy difference. The Helmholtz energy difference between two subensembles is given by

$$\beta A_j - \beta A_i = w_j - w_i - \ln(P_j/P_i) \quad (5)$$

where  $P_i$  is the probability of observing the system associated with

$\lambda_i$  during the simulation. In general, subensembles corresponding to intermediate values of the coupling parameter are not of physical significance, but they play a role of providing a smooth path in the configuration space between the two end systems of physical interest. The chemical potential of a solute molecule in excess of that of an ideal gas at the same temperature and density is given by

$$\beta \mu^{ex} = w_M - w_0 - \ln(P_M/P_0) \quad (6)$$

From computational point of view, obtaining a good set of the weight factors is of importance. Ideally, optimal value is the free energy itself (in units of kT) that would make the probability  $P_i$  completely uniform. If one uses poor weight factors, certain subensembles might not be visited within finite simulation time, which results in a divergence problem caused by zero probability. While Eq. (5) can be successively used to refine weights in preliminary simulations as has been done in the previous simulation studies, it is often a tedious task requiring many trial-and-error attempts. As in our previous work [19], we use the more robust method to adaptively determine the weight factors during the simulation. With a current value of w (initially set to zero), the acceptance ratios for forward and backward transitions gives a new value of w by

$$w^{new} = w^{old} - \ln(\overline{P_{acc}^f}/\overline{P_{acc}^b}) \quad (7)$$

Updating the weight factor with Eq. (7) is iteratively done until a convergence is obtained. The convergence signifies that the two acceptance ratios become equal to each other,  $\overline{P_{acc}^f} = \overline{P_{acc}^b}$ . More details of the algorithm and discussions about its implementation are referred to our previous work.

## RESULTS AND DISCUSSION

Pure solvent phases consisting of 300 carbon dioxide molecules were first prepared by carrying out isothermal isobaric Monte Carlo (NPT MC) simulations at 300, 325 and 350 K with pressures ranging from 10 to 500 bar. The lowest temperature of 300 K is slightly below the critical temperature of carbon dioxide, 304 K. Simulation results for specific volume of carbon dioxide are shown in Table 1. Simulation uncertainties are less than 0.1%. In Fig. 1, the values of specific volumes are compared with experimental data [25] and values predicted by the Peng-Robinson (PR) equation of state [26,27].

**Table 1. NPT Monte Carlo simulation results for PVT properties of carbon dioxide. Numbers are specific volume in units of cm<sup>3</sup>g<sup>-1</sup>. Simulation uncertainties for the specific volume are less than 0.1%**

Pressure (bar)	Temperature (K)		
	300	325	350
10	54.4	59.6	64.7
20	25.9	28.7	31.5
40	11.4	13.2	14.9
100	1.31	3.44	4.73
200	1.12	1.34	1.74
300	1.06	1.19	1.36
400	1.02	1.11	1.23
500	0.986	1.06	1.16

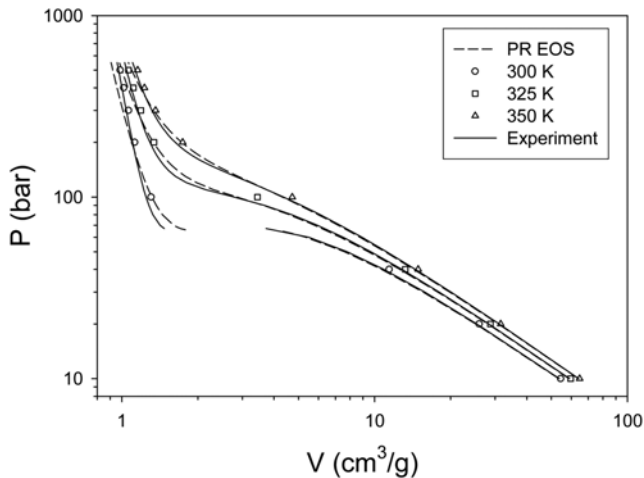


**Fig. 1.** PVT properties of carbon dioxide. Symbols are results from Monte Carlo simulations, dashed lines are the predictions of Peng-Robinson equation of state, and solid lines are experimental data [25].

Agreement between simulations and experiment is satisfactory, while simulation tends to slightly overestimate the specific volume. The predictions of the PR equation of state and experimental data are nearly the same for gas phase up to the critical density, but somewhat deviate for compressed liquids and supercritical conditions. For pressures higher than 300 bar, the PR equation of state predicts smaller specific volumes than experimental data, while a good agreement is seen between experimental data and MC simulation results. This is because the repulsion term of the PR equation of state is valid only for low densities (drawback inherited by the van der Waals equation of state). In contrast, MC simulations with realistic molecular model yield accurate PVT data even for high pressures and liquid-like densities.

The excess chemical potentials of carbon dioxide and hydrocarbon solutes at infinite dilution were calculated by EEMC simulations. Simulations were performed at 300 and 350 K and at constant volume conditions that corresponds to 40, 100, 300 and 500 bar, respectively. Each EEMC simulation was run for  $2.5 \times 10^7$  MC cycles. Simulation results for the excess chemical potentials are listed in Table 2. The numbers in parentheses are simulation uncertainties in last digits that were taken as standard deviations over five block averages. The numbers in superscripts are the number of steps in coupling parameter  $\lambda$ . The number of steps in  $\lambda$  or the number of subensembles can be optimally chosen so as to minimize uncertainty of simulation results. If too many steps are used, most of computer time will be spent on ‘unphysical’ intermediate subensembles. If the number of intermediate subensembles is too less, transitions between subensembles will not be accepted frequently enough to give accurate simulation results. We choose the number of steps such that overall acceptance ratio for  $\lambda$  transitions should be greater than at least 15%.

In Fig. 2, the excess chemical potentials of carbon dioxide are compared with experimental values as well as the predictions of the PR equation of state. Their values decrease with the increasing pressure for low-pressure gas phase, but become increasing with the pressure for compressed phases. Note that the excess chemical

**Table 2.** Expanded ensemble Monte Carlo simulation results for the excess chemical potentials of solutes dissolved in carbon dioxide at infinite dilution. Values are in units of kJ mol<sup>-1</sup> and numbers in parenthesis are simulation uncertainties in last digits. Numbers in superscripts are the number of steps in coupling parameter. Results for carbon dioxide are compared with experimental values

Solute	Pressure (bar)	Temperature (K)	
		300	350
Carbon dioxide	40	-0.997 (3) <sup>1</sup>	-0.629 (5) <sup>1</sup>
		-1.173 *	-0.720 *
	100	-5.259 (15) <sup>4</sup>	-1.779 (8) <sup>1</sup>
		-5.539 *	-2.107 *
	300	-4.739 (28) <sup>4</sup>	-3.599 (35) <sup>4</sup>
		-5.006 *	-3.870 *
Methane	40	-0.594 (2) <sup>1</sup>	-0.367 (3) <sup>1</sup>
		-2.312 (19) <sup>2</sup>	-0.999 (4) <sup>1</sup>
	500	0.039 (51) <sup>4</sup>	0.092 (35) <sup>4</sup>
	40	-1.137 (3) <sup>1</sup>	-0.737 (4) <sup>1</sup>
		-5.658 (43) <sup>4</sup>	-2.073 (8) <sup>1</sup>
Ethane	500	-3.299 (26) <sup>4</sup>	-2.791 (20) <sup>4</sup>
	40	-2.083 (7) <sup>1</sup>	-1.349 (4) <sup>1</sup>
		-10.694 (47) <sup>4</sup>	-3.845 (9) <sup>1</sup>
	100	-7.503 (104) <sup>5</sup>	-6.331 (39) <sup>5</sup>
n-Hexane	40	-3.083 (7) <sup>1</sup>	-1.982 (6) <sup>1</sup>
		-15.515 (54) <sup>5</sup>	-5.595 (17) <sup>1</sup>
	500	-11.580 (79) <sup>8</sup>	-9.808 (53) <sup>8</sup>
	100	-4.095 (10) <sup>1</sup>	-2.619 (7) <sup>1</sup>
		-20.175 (58) <sup>8</sup>	-7.365 (20) <sup>1</sup>
n-Octane	500	-15.129 (66) <sup>8</sup>	-12.913 (74) <sup>8</sup>
	40	-2.754 (3) <sup>1</sup>	-1.793 (5) <sup>1</sup>
		-14.636 (52) <sup>5</sup>	-5.150 (24) <sup>1</sup>
	100	-12.593 (74) <sup>8</sup>	-10.643 (30) <sup>8</sup>
Benzene	40	-3.299 (6) <sup>1</sup>	-2.134 (5) <sup>1</sup>
		-17.075 (73) <sup>8</sup>	-6.086 (16) <sup>1</sup>
	500	-14.499 (90) <sup>8</sup>	-12.225 (59) <sup>8</sup>
	100		
Toluene	40		
	100		
	500		

\*Calculated from experimental data [25]

potential is related to fugacity by

$$\mu^{ex} = RT \ln(f/\rho RT) \quad (8)$$

where  $f$  is the fugacity,  $\rho$  is the molar density of CO<sub>2</sub> and R is the gas constant [12]. Compared with experimental data, MC simulation predicts a little higher value of the chemical potential, whereas the PR equation of state gives lower values except for the region close to the critical point. For compressed phases, the chemical potentials at pressures higher than 500 bar appear to be more accurately predicted by EEMC simulations than the PR equation of state. A systematic overestimation of EPM2 model for the chemical potential is mainly due to the overestimation of specific volume. Recalling that the chemical potential is related to an integral of specific

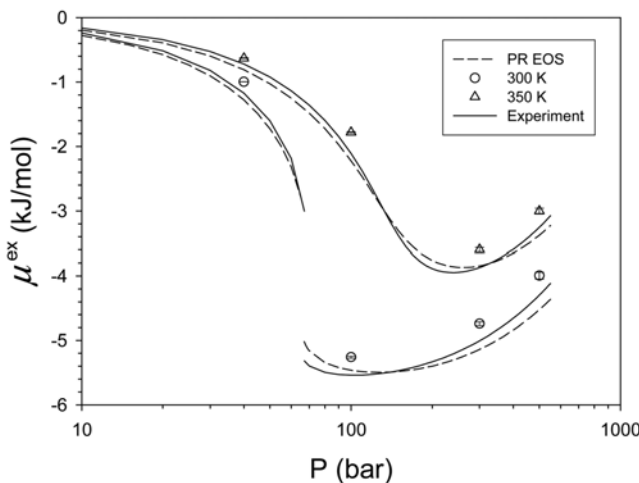


**Fig. 2.** The excess chemical potential of carbon dioxide. Lines and symbols have the same meanings as in Fig. 1.

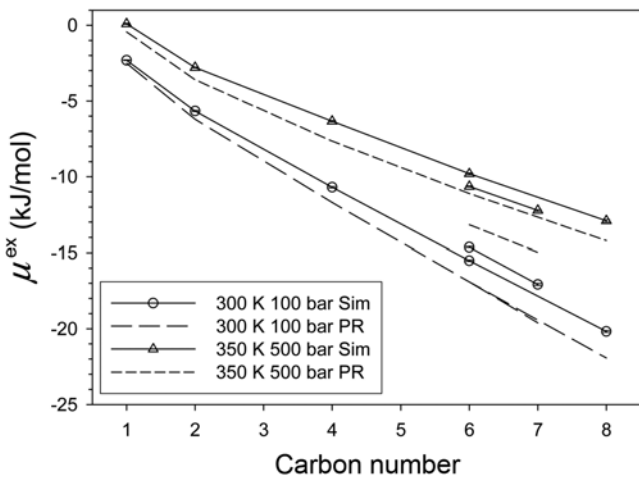


**Fig. 3.** The excess chemical potential of hydrocarbon solutes in carbon dioxide at infinite dilution. Symbols are results from Monte Carlo simulations, solid lines are eye-guides and dashed lines are the predictions of Peng-Robinson equation of state. Separate data are for aromatic compounds.

volume over the pressure, small systematic errors for PVT properties would result in more pronounced errors for chemical potential or fugacity.

The excess chemical potentials of hydrocarbon solutes at infinite dilution obtained from EEMC simulations are shown in Table 2. Results for two compressed conditions are plotted in Fig. 3 with respect to the carbon number of the solute molecules: one at 300 K and 100 bar with the specific volume of  $1.31 \text{ cm}^3 \text{g}^{-1}$  and the other at 350 K and 500 bar with  $1.16 \text{ cm}^3 \text{g}^{-1}$ . The magnitudes of the excess chemical potentials become larger with the chain length: the longer the chains, the stronger the dispersion interactions. Almost linear dependence with chain length was observed except for methane with chain-end effect. As experimental data for the excess chemical potentials are not readily available, we compare simulation results with the predictions of the PR equation of state without binary interaction parameter. Similarly to Eq. (8), the excess chemical poten-

tial at infinite dilution is related to the fugacity by

$$\mu_2^{\text{ex},\infty} = \lim_{x_2 \rightarrow 0} RT \ln(f_2/x_2 \rho_1 RT) \quad (9)$$

where subscripts 1 and 2 denote solvent and solute, respectively. The predicted values of the chemical potential from the PR equation of state are lower than those from simulations, and this tendency is the same as with carbon dioxide. For aromatic compounds of benzene and toluene, simulations predict slightly higher values at 300 K and somewhat lower values at 350 K. This is consistent with the predictions of the PR equation of state with minor quantitative differences. As can be seen in Table 3, the comparison of results between 300 and 350 K at the same pressure of 500 bar shows that lowering temperature significantly decreases the excess chemical potential. Since the excess chemical potential is a thermodynamic measure of the solvent-solute affinity, the present simulation study explains the feasibility of supercritical extraction process at molecular level: Extraction of nonpolar hydrocarbons by carbon dioxide will be thermodynamically favored at lower temperature. In reality, however, there must be compromise with other rate processes such as diffusion and mixing.

## CONCLUSIONS

We find that expanded ensemble Monte Carlo simulations provide an accurate and useful tool to directly calculate the chemical potentials of carbon dioxide and hydrocarbon solutes at high pressures. Unlike other simulation schemes, the EEMC simulation allows for chemical potentials to be obtained from a single run of simulation, and the adaptive method provides a convenient and robust way of finding weight factors on the fly. Less than eight intermediate states are required to insert (or delete) hydrocarbon solute molecules (up to n-octane) into dense  $\text{CO}_2$  phase of approximately  $1.0 \text{ g cm}^{-3}$ . The excess chemical potentials obtained from EEMC simulations are as accurate as the predictions of the PR equation of state for low and intermediate pressures, and outperform the PR equation of state at high pressure of 500 bar. This is because molecular simulations use realistic molecular model resulting in accurate PVT data even for high pressures and liquid-like densities. Unlike the PR equation of state, molecular simulation does not require adjustable binary interaction parameter, and its usefulness would be much appreciated for mixtures of nonpolar and polar compounds.

## ACKNOWLEDGEMENT

This work was supported by the Korea Research Foundation Grant funded by the Korean Government (MOEHRD, Basic Research Promotion Fund) KRF-2008-313-D00185.

## NOMENCLATURE

A	: Helmholtz energy
f	: fugacity
N	: number of molecules
k	: Boltzmann constant
P	: pressure
$P_i$	: probability of observing the system i

Q	: canonical partition function
q	: partial charge
R	: gas constant
r	: distance
U	: potential energy
u	: interatomic potential energy
V	: specific volume
T	: temperature
w	: weight factor
x	: mole fraction

**Greek Letters**

$\beta$	: inverse of kT
$\varepsilon$	: Lennard-Jones energy parameter
$\varepsilon_0$	: permittivity of vacuum
$\lambda$	: coupling parameter
$\mu$	: chemical potential
$\rho$	: molar density
$\sigma$	: Lennard-Jones size parameter

**Superscripts**

b	: backward
ex	: excess
f	: forward
intra	: intramolecular

**Subscripts**

acc	: acceptance
-----	--------------

**REFERENCES**

1. D. Frenkel and B. Smit, *Understanding Molecular Simulations 2nd Ed.*, Academic, San Diego (2002).
2. B. Widom, *J. Chem. Phys.*, **39**, 2808 (1963).
3. R. W. Zwanzig, *J. Chem. Phys.*, **22**, 1420 (1954).
4. J. G. Kirkwood, *J. Chem. Phys.*, **3**, 300 (1935).
5. C. H. Bennett, *J. Comput. Phys.*, **22**, 245 (1976).
6. A. P. Lyubartsev, A. A. Martsinovski, S. V. Shevkunov and P. N. Vorontsov-Vel'yaminov, *J. Chem. Phys.*, **96**, 1776 (1992).
7. A. P. Lyubartsev, A. Laaksonen and P. N. Vorontsov-Velyaminov, *Mol. Phys.*, **82**, 455 (1994).
8. A. P. Lyubartsev, A. Laaksonen and P. N. Vorontsov-Velyaminov, *Mol. Simul.*, **18**, 455 (1996).
9. A. P. Lyubartsev, S. P. Jacobsson, G. Sundholm and A. Laaksonen, *J. Phys. Chem. B*, **105**, 7775 (2001).
10. J. R. Errington, G C. Boulougouris, I. G. Economou, A. Z. Panagiotopoulos and D. N. Theodorou, *J. Phys. Chem. B*, **102**, 8865 (1998).
11. G C. Boulougouris, J. R. Errington, I. G. Economou, A. Z. Panagiotopoulos and D. N. Theodorou, *J. Phys. Chem. B*, **104**, 4958 (2000).
12. A. A. Khare and G. C. Rutledge, *J. Chem. Phys.*, **110**, 3063 (1999).
13. A. A. Khare and G. C. Rutledge, *J. Phys. Chem. B*, **104**, 3639 (2000).
14. K. M. Åberg, A. P. Lyubartsev, S. P. Jacobsson and A. Laaksonen, *J. Chem. Phys.*, **120**, 3770 (2004).
15. J. Chang and S. I. Sandler, *J. Chem. Phys.*, **118**, 8390 (2003).
16. J. Chang, A. M. Lenhoff and S. I. Sandler, *J. Chem. Phys.*, **120**, 3003 (2004).
17. J. Chang, A. M. Lenhoff and S. I. Sandler, *J. Phys. Chem. B*, **109**, 19507 (2005).
18. J. Chang and S. I. Sandler, *J. Chem. Phys.*, **125**, 054705 (2006).
19. J. Chang, *J. Chem. Phys.*, **131**, 074103 (2009).
20. J. G. Harris and K. H. Yung, *J. Phys. Chem.*, **99** 12021 (1995).
21. J. Vorholz, V. I. Harismiadis, B. Rumpf, A. Z. Panagiotopoulos and G. Maurer, *Fluid Phase Equilibria*, **170**, 203 (2000).
22. M. G. Martin and J. I. Siepmann, *J. Phys. Chem. B*, **102**, 2569 (1998).
23. C. D. Wick, M. G. Martin and J. I. Siepmann, *J. Phys. Chem. B*, **104**, 8008 (2000).
24. B. Chen, J. J. Potoff and J. I. Siepmann, *J. Phys. Chem. B*, **105**, 3093 (2001).
25. E. W. Lemmon, M. O. McLinden and D. G. Friend, "Thermophysical Properties of Fluid Systems" in NIST Chemistry WebBook, NIST Standard Reference Database Number 69, Eds. P. J. Linstrom and W. G. Mallard, National Institute of Standards and Technology, Gaithersburg MD, 20899, <http://webbook.nist.gov> (retrieved April 10, 2010).
26. D.-Y. Peng and D. B. Robinson, *Ind. Eng. Chem. Fundam.*, **15**, 59 (1976).
27. S. I. Sandler, Chemical, Biochemical and Engineering Thermodynamics 4th Ed., John Wiley & Sons (2006).